1949 BIENNIAL INSPECTION (BROWN)

COMPRESSIBLE FLOW UNIT

THE SUBJECT OF THIS TALK IS THE PROBLEM OF OBTAINING HIGH LIFT DRAG RATIOS AT SUPERSONIC SPEEDS.

One of the major efforts of aeronautical research must always be directed toward the attainment of higher aerodynamic efficiencies of flight. The attainment of increased efficiencies of flight is especially important at supersonic speeds where additional drag arising from the formation of shock waves tends to reduce the lift drag ratios below those obtainable at subsonic speeds. There are several factors which influence the lift drag ratio, most important of which are: (1) lift coefficient (2) wing planform (3) wing thickness ratio. It is obviously desirable to operate an airplane or missile at its maximum lift drag ratio; this cannot be done, however, unless the altitude and wing loading are properly adjusted for flight at the correct attitude. To illustrate this effect a chart has been prepared showing the variation of altitude with wing loading for a typical configuration. The lift coefficient for $(L/D)_{max}$ at M = 1.4 was taken as .25 corresponding to an angle of attack of about 6°. As the attitude of the aircraft fixes its (L/D) independent of the altitude, it can be understood that the lift developed will depend on the ambient pressure. At sea level therefore, the lift will be great, and for the typical conditions chosen would correspond to a wing loading of 740 lbs per sq. foot. Obviously such high wing loadings rule out the possibility of using maximum lift drag ratios except perhaps on missiles having mild maneuverability requirements. A configuration designed for max L/D at 10,000 feet would look similar to the sketch shown on the right of the chart. With the required wing loading of 500 the aircraft would be incapable of landing. More reasonable configurations from the landing standpoint would have wing loadings close to those currently used on high speed subsonic aircraft. The upper limit of

100 represents a landing condition at sea level of 200 mph with a lift coefficient of 1.0. A configuration with a wing loading of 100 would look similar to the sketch on the left of the chart. It can be seen the aircraft must go to great altitudes to obtain the angle of attack for max (L/D) in level flight. Unfortunately, present day turbo-jet power plants are unable to maintain high thrusts at high altitudes and hence the high altitude aircraft would be penalized severely in power plant weight and size and also in the size of air inlets required.

In the usual airplane design problem, the wing loading is fixed by the landing condition and the altitude by the operational requirements, hence the lift coefficient of flight is fixed. For example, high speed low altitude fighters or research airplanes would be required to fly at very low lift coefficients by low speed landing requirements and would not necessarily have high maximum lift drag ratios. In fact, the most important factor for these aircraft would be low minimum drag coefficients, as the drag due to lift would be very small and unimportant in its effect on the lift drag ratio. A theoretical analysis has been made to illustrate the relative merits at various wing planforms on a given fuselage. The analysis will be discussed first on the basis of maximum drag and second on the basis of $(L/D)_{max}$. In the analysis, three general types of wing planforms were considered: swept-back or arrow wings, delta wings, and unswept tapered wings. A simple structural criterion was introduced to obtain a variation in airfoil thickness ratio with planform. The wing loadings were held constant and suitable skin friction factors were added. The study shown is an extension on the work of R. T. Jones presented at past inspections and uses his assumptions in order to provide a fair comparison of the various planforms.

On this first chart are presented the C_D minimum curves for the arrow, triangular, and two tapered unswept wings. The computations include the drag of a fuselage and tail surface and therefore represent expected values of the drag coefficient. It may be seen that for comparable aspect ratios there is little difference between the various planforms. In general the low aspect ratios are probably the best choice for low altitude high speed aircraft, although it should be emphasized that other factors such as torsional stiffness, stability, and landing ability have not been considered in the analysis. It appears that the choice of wing planform will be dictated by conditions in ranges of velocity other than the supersonic. The effect of planform on landing ability or stability in the transonic flight range is therefore of the same importance as the high speed characteristics in the aircraft design.

The second chart shows the same wings compared on the basis of maximum lift-drag ratio. Here there is a reversal of the effects shown on Slide II. The arrow type planform shows a definite superiority over the other planforms, and hence would be an obvious choice where maximum lift drag ratios may be utilized. It should be noted that the $C_{D_{o_{min}}}$ values represent a design criterion for lift coefficients approaching zero and the $(L/D)_{max}$ values represent a criterion for lift coefficients approaching $C_{L_{optimum}}$ and that these are both extremes in a design sense.

In regard to the highly swept arrow and delta wings, preliminary experiments have shown the desirability of camber if high lift drag ratios are to be obtained. The camber is used, as in subsonic flow, to produce pressure distributions more favorable to the boundary layers. Chart III

has been prepared to illustrate the difference in calculated loading between a flat and a cambered delta wing. It will be seen that the flat wing produces a low pressure peak at the leading edge followed by a very high adverse pressure gradient. This type of pressure distribution is typical of uncambered wings having subsonic leading edges, that is, wings on which the stream velocity component normal to the leading edge is less than the sonic speed. Cambering the delta wing to give uniform loading as shown on the right of the chart required rather high section angles of attack at the root. These high angles at the root, or the high degree of twist requires is illustrated in the model. It may be that camber applied only to the leading edges would produce a more practical wing design. A uniformly loaded wing should, therefore, be considered as an extreme case and is not necessarily intended to represent the best configuration, but rather should be considered as a first step in any investigation of camber effects.

In conclusion, it appears on the basis of experimental evidence so far accumulated from relatively low-scale experiments, that the effects of camber in improving the flow in the boundary layer over wings have been realized. The extent to which these beneficial effects of camber will be realized for full scale supersonic aircraft can only be determined from experiments which permit a large variation in the Reynolds number.

(Discussed by Mr. K. R. Czarnecki and Mr. E. E. Ulmann at the Compressible Flow Unit during the 1949 Biennial Inspection)

FLAPPED SUPERSONIC AIRFOILS

Introduction

Existing data on flapped supersonic airfoils have come chiefly from small wind tunnels operating at low Reynolds numbers. Large viscous effects arising from shock-boundary layer interactions are evident in these small-scale tests.

During the past year tests of flapped supersonic airfoils were made at higher Reynolds numbers and Mach numbers than have previously been attained to determine the importance of viscous effects at conditions approximating full-scale for some missile configurations.

Chart I

(* Indicates that the speaker points to the appropriate part of the chart under discussion)

These are photographs at Mach numbers of 1.6 and 4.0 * of the flow around a three-dimensional flapped wing having a 9-percent thick symmetrical circular-arc airfoil section, and a 30-percent chord trailing edge flap. As may be obvious from the difference in character of the pictures on the two sides of the chart, the data presented here were obtained in two of the Laboratory's supersonic facilities, the nine-inch supersonic tunnel and the nine-inch Mach No. 4 jet which operates for short periods of time with settling chamber pressures up to 250 pounds per square inch.

The test Reynolds numbers were 1 million at Mach number 1.6 and five times that or 5 million at M = 4.0. These * are the struts supporting the models. The struts are shaped so that the flow over the lower surface of the models will not be greatly disturbed.

The main features of the flow over the wing can be determined from the position and shape of the shocks and expansions. Shocks generally appear as dark lines * (pointing to M - 4 photo) while expansions appear as light regions * in the photographs.

In these pictures, for example, * (M - 1.6 pictures) the upward flap deflection causes a double or forked shock to form on the upper surface. This leg * of the double shock indicates that the flow has separated from the airfoil surface ahead of the flap hinge line at this point. *.

In contrast to this picture * (upper left) the picture at the higher Mach number and Reynolds number condition * (upper right) shows no sign of separation on the upper surface. This change in flow conditions is primarily a scale effect brought about by the increase in Reynolds number from one million * to five million.

Chart II

This chart presents the pressure distribution for a typical wing-flap configuration. The illustration * is a composite photograph showing undisturbed flow on both surfaces of the airfoil. On the corresponding pressure distribution diagram, the theoretical pressure distribution is indicated by the dashed red line and the experimental distribution by the solid black line with symbols.*

The large degree of separation from the lower surface seen here * indicates a serious discrepancy between the theoretically assumed and experimental flows. However, the pressure distribution shows that the practical effects of this discrepancy are small because the maximum negative pressure that can occur over this surface * is a complete vacuum, which

corresponds to this relatively small negative pressure coefficient. ~~Thus, complete separation at the flap hinge line on the low pressure surface decreases flap effectiveness very little;~~ Therefore, flap effectiveness at this high Mach number is dependent almost entirely upon the pressures on the high pressure surface of the flap.

Integration of pressure distributions obtained from systematic tests yielded the airfoil characteristics, some of which are presented on the next chart.

Chart III

The airfoil characteristics presented here are for an angle of attack of 2 degrees.

These three figures * indicate that flap effectiveness and drag were found to agree fairly well with the theoretically predicted values at a Mach number of 4.

The lower figures * show hinge moment curves for the same airfoil section at two Mach numbers and Reynolds numbers. At the low Mach number and Reynolds number condition the hinge moment curve shows a region of about 3 degrees * where changing the flap angle causes no change in hinge moment. This phenomenon disappears at the higher Reynolds number and Mach number condition as is shown by this curve * (lower left).

Thus it is seen that Reynolds number is an important variable in supersonic flow, and that the results obtained at low Reynolds numbers may not be applicable at flight Reynolds numbers. Therefore high Reynolds number data is just as necessary at supersonic speeds as it is at subsonic speeds.

From these figures it can also be seen that the shock expansion theory gives a fairly accurate prediction of the forces on the two-dimensional section of a flapped circular-arc airfoil in this Reynolds number range. However, in the region of the wing tip the agreement between theory and experiment is not so good.

Chart IV

On this chart * are presented the theoretical and experimental pressure distributions at a section of the wing near the tip * (pointing to planform diagram). The angle of attack is 4.35 degrees * and the flap angle is -12 degrees * . The best available theory predicts the pressure distribution shown by the red and green lines * , while the black lines with symbols indicate the experimental pressure distribution. The disagreement over the flap surface is quite apparent. It can be seen, therefore, that extensive research remains to be accomplished to determine the forces in these regions of the wing where the theory is not adequate.

1949 BIENNIAL INSPECTION

COMPRESSIBLE FLOW UNIT

SUPERSONIC COMPRESSOR AERODYNAMICS

Many important advances in gas turbine engines have had their origin in aerodynamic research utilizing stationary cascades representing the blade rows of compressors or turbines. Supersonic cascade investigations were initiated at this Laboratory in 1944. The results of this work made possible the design of the first successful axial-flow supersonic compressor. This machine was developed and tested in 1945 and was discussed at the 1946 inspection of this Laboratory. Since that time, supersonic cascade research has been continued and has led to a number of improvements in the original type of supersonic compressor, and recently has provided the basic information for the design of an entirely new type of supersonic compressor.

Basic cascade research is necessarily followed by tests of actual rotors to investigate three-dimensional effects and to obtain a precise evaluation of rotor performance. The original (type 1) shock-in-rotor compressor shown here has very thin blades (thickness chord ratio of 2 percent) requiring the presence of a shroud. The performance of this rotor as tested in Freon at this Laboratory is shown on the first chart. This design was later tested in air at the Lewis Laboratory where research on supersonic compressors is also under way. This chart also shows for comparison the relatively low pressure rises per stage obtainable in the best experimental

subsonic axial-flow design. This first rotor, while not practical, did verify many of the assumptions made in its design. This made possible the development of a second rotor of blade sections sufficiently thick to prevent vibration without the use of a shroud. Its performance is shown in the first chart. This rotor and two more recent designs, which have evolved from additional cascade studies, are mounted on this table. It will be noted that pressure rise per stage is approaching the practical limit for type-1 compressors.

Although it is not yet four years since the operation of the first supersonic compressor, a practical turbo-jet engine incorporating a supersonic axial-flow compressor has been built by an engine manufacturer. In preliminary tests, this compressor has equalled expectations.

Further research upon type-1 compressors is expected to yield improvements of diminishing returns as acceptable three-dimensional flow theories are advanced. However, impulse designs in which the static pressure rise occurs in the stator, offer interesting possibilities for a radical increase of pressure ratio per stage. This was shown in a 1946 NACA Report by Kantrowitz and, later, in the Institute of Aeronautical Sciences Journal by Wattendorf.

To illustrate the differences, a typical velocity diagram for the original and impulse compressors are shown on these

charts. The entering conditions and rotor speeds are identical with those of type-1; however, within the rotor, the flow is entirely supersonic. The air is turned through a considerable angle in the rotor and enters the stator at a Mach number of 2.5.

The major aerodynamic design problems of this type compressor are: (1) rotor blades to turn the air through large angles at supersonic speeds; (2) stator blades to efficiently convert the supersonic flow energy to static pressure; and (3) the effect of three-dimensional cross flows within the blade passages. The first two problems can readily be studied in cascades.

Preliminary cascade investigations have proven the feasibility of the impulse compressor. As can be seen in chart, air has been turned supersonically (a full 90° in this case) at an entering Mach number of 1.70. The loss in total pressure, which includes oblique shock and frictional losses, is only five percent.

The supersonic portion of such a stator can be seen. The movable leading edge has been deflected to increase the supersonic compression after the flow has started. This particular diffuser has successfully converted 75 percent of the kinetic energy of stream to static pressure at an inlet Mach number of 2.5

To study the three-dimensional effects mentioned before, a single-stage compressor is being built. This compressor has been designed using information obtained from two-dimensional cascade tests. The three-dimensional effects are unpredictable; however, if no large adverse effects occur, it is estimated from cascade results that a pressure ratio of 8 at an efficiency of 80 percent should be obtained.

A single impulse supersonic compressor would replace eight stages similar to the experimental subsonic stage previously mentioned (point), or 12 rotors and stators of currently used subsonic compressors.

Using this (point) compressor, very compact, light-weight, Jet-Propulsion engines could be constructed. It is to this goal that this work is directed.

NACA

LAL 61100

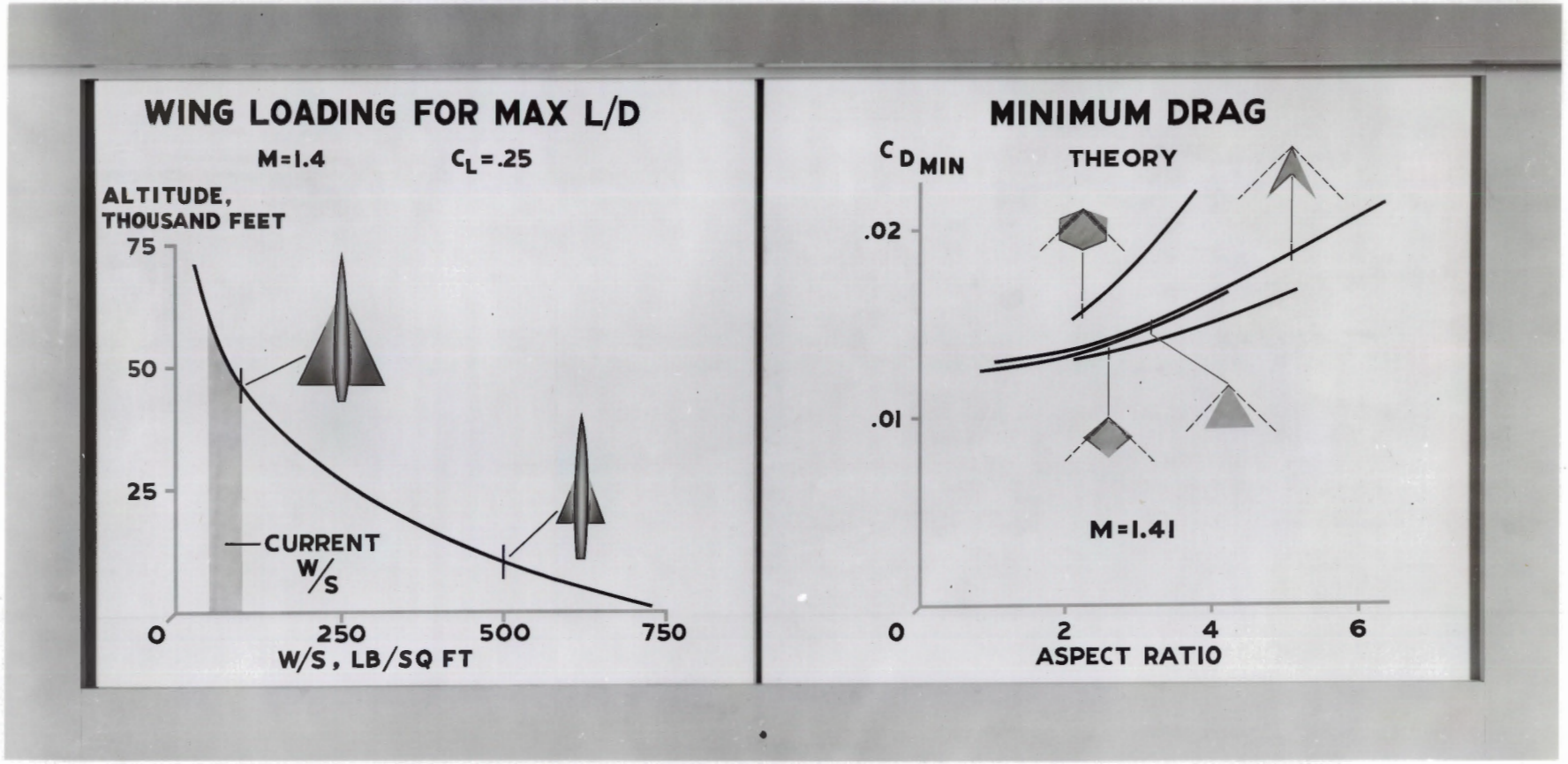

NACA

LAL 61101

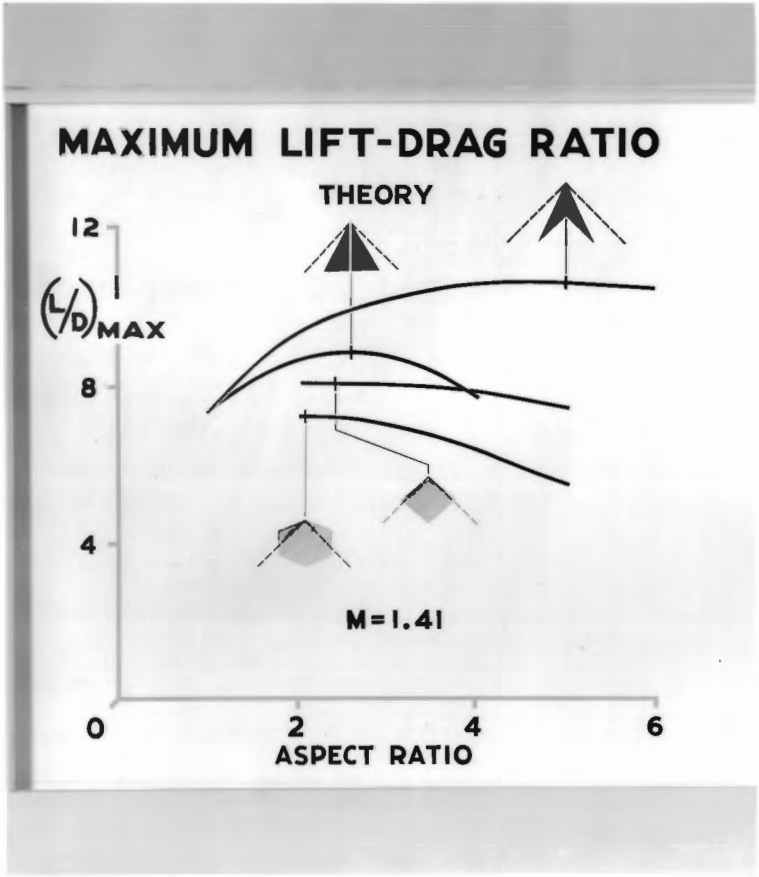

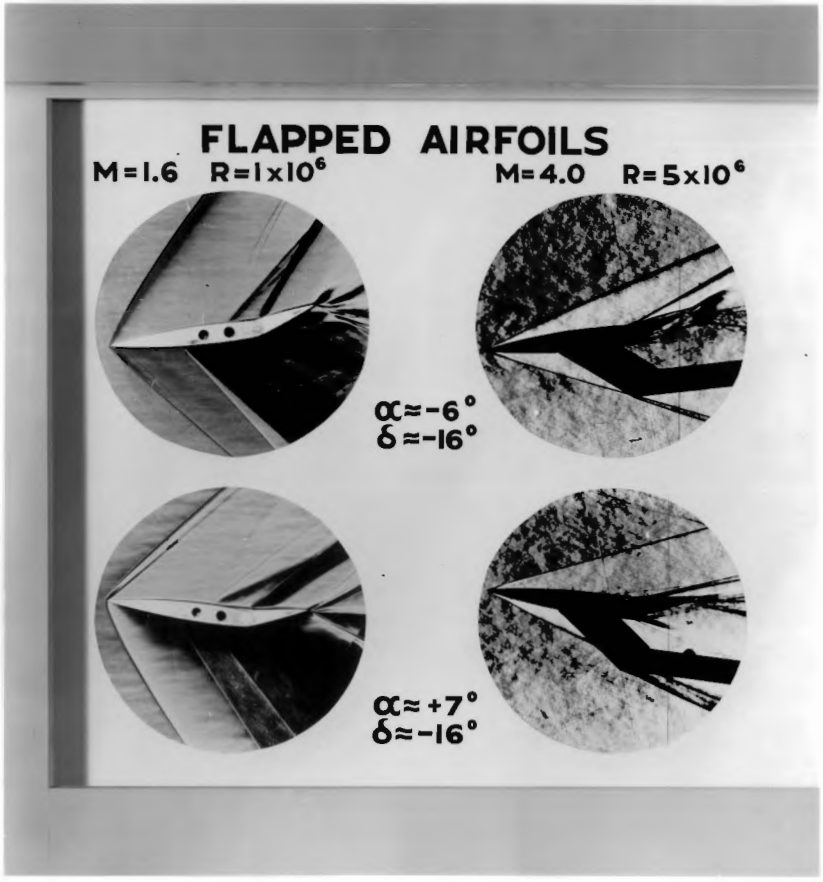

NACA

LAL 61102

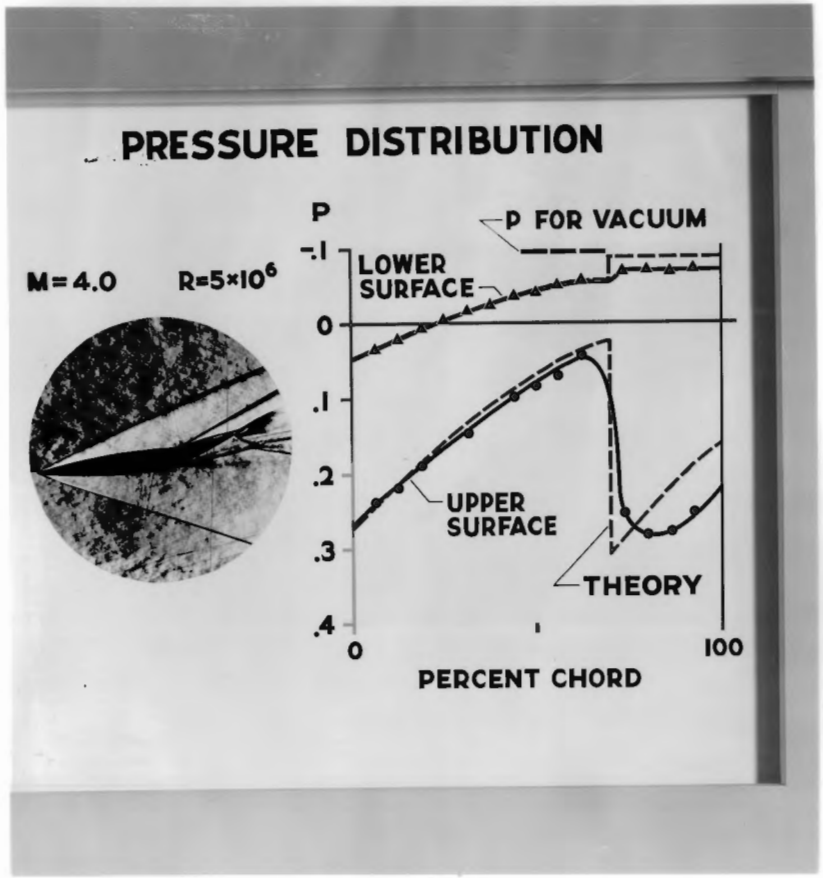

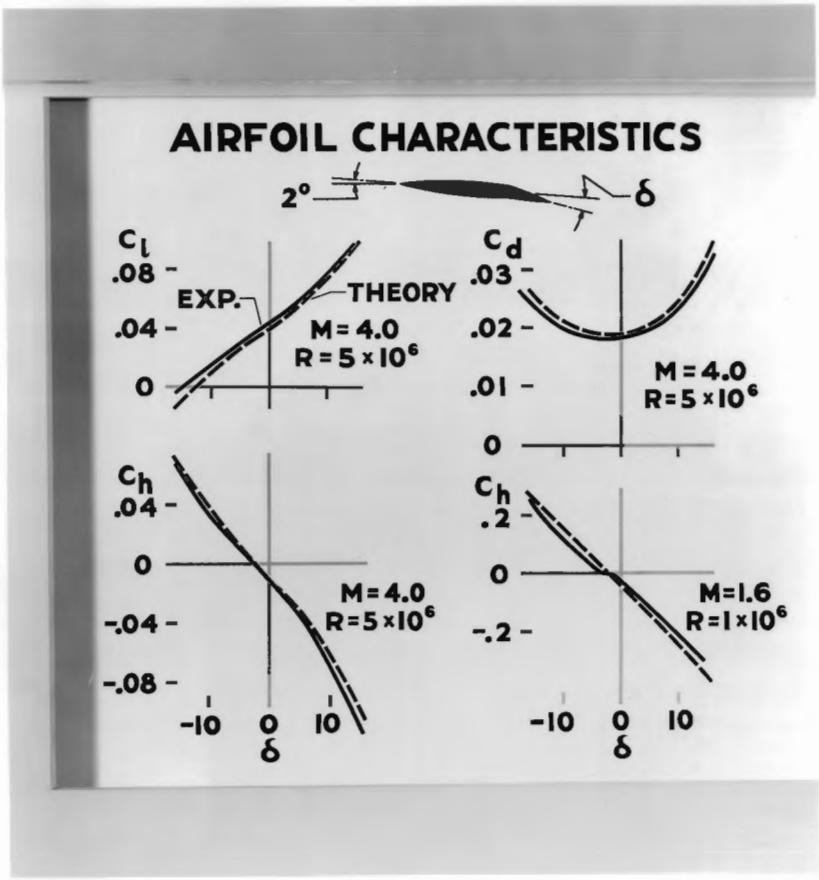

NACA

LAL 61103

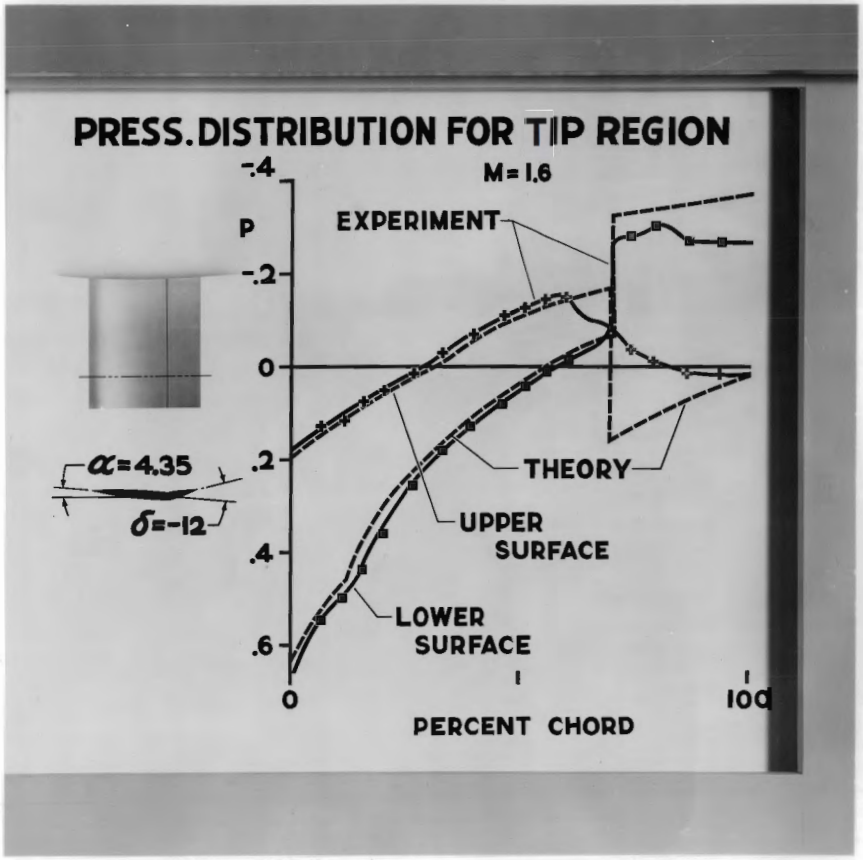

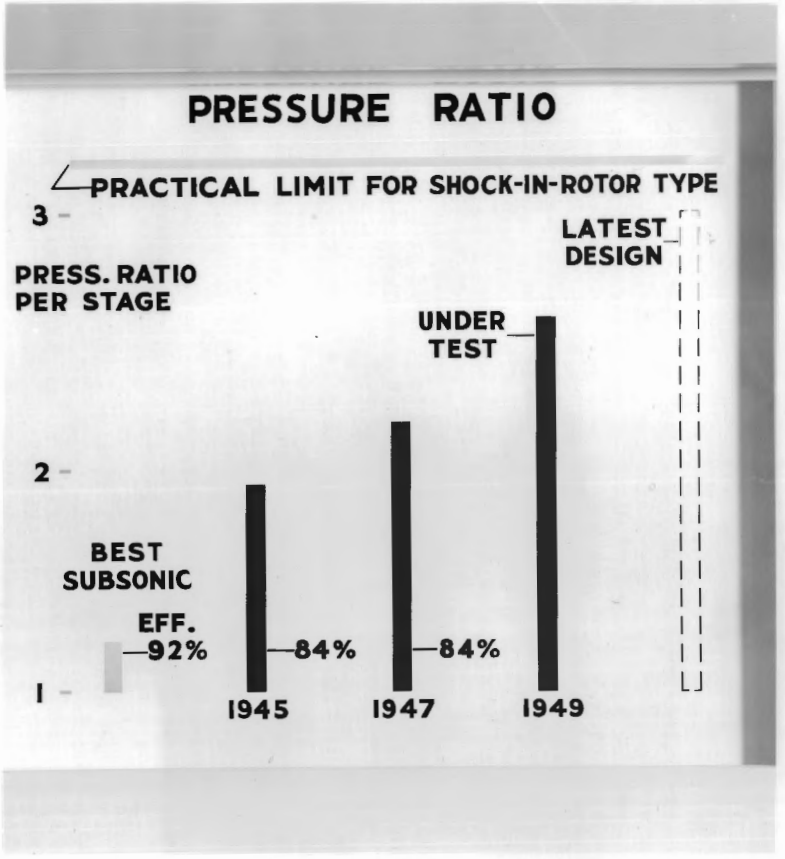

NACA

LAL 61104

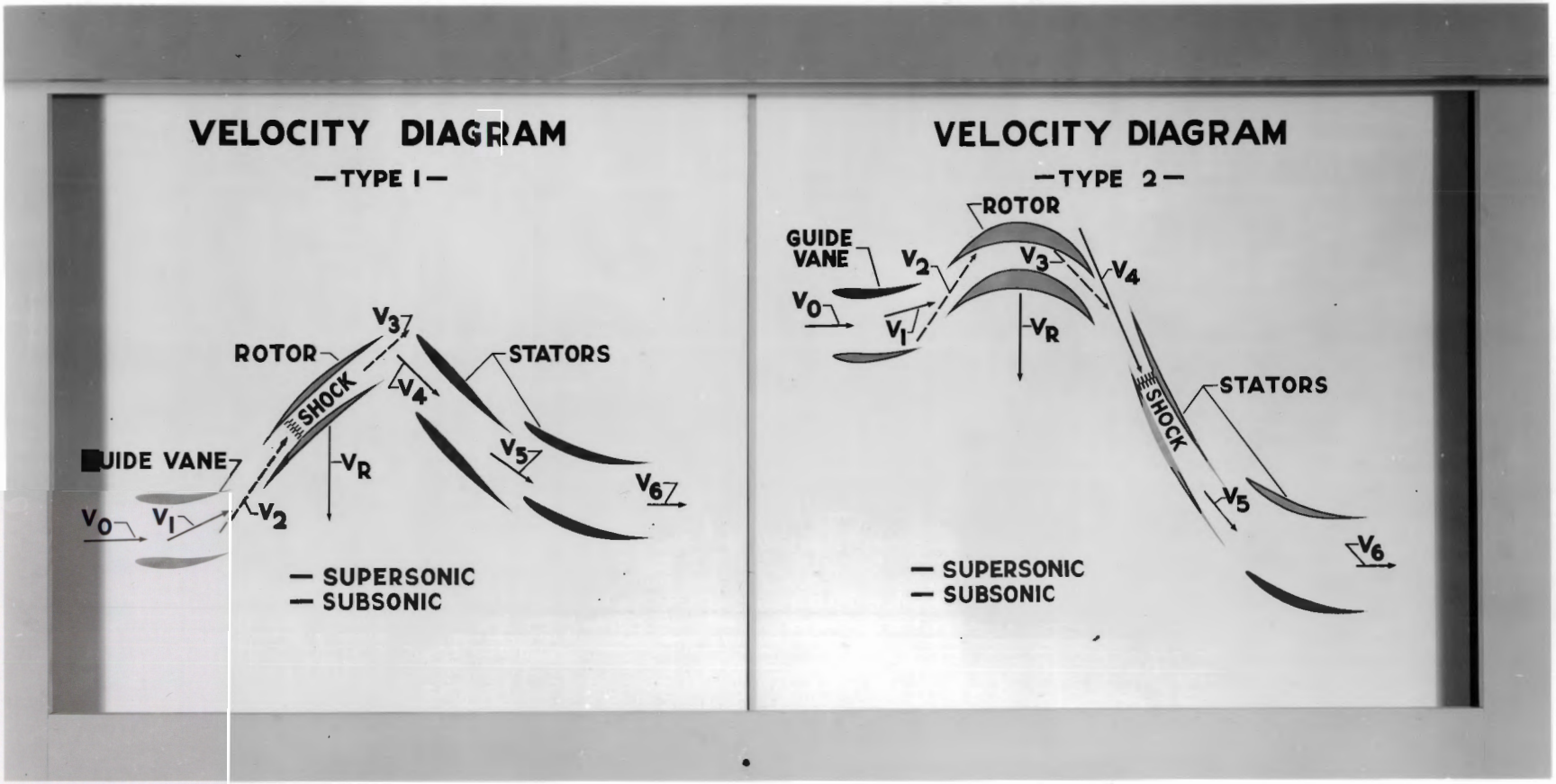

NACA

LAL 61105

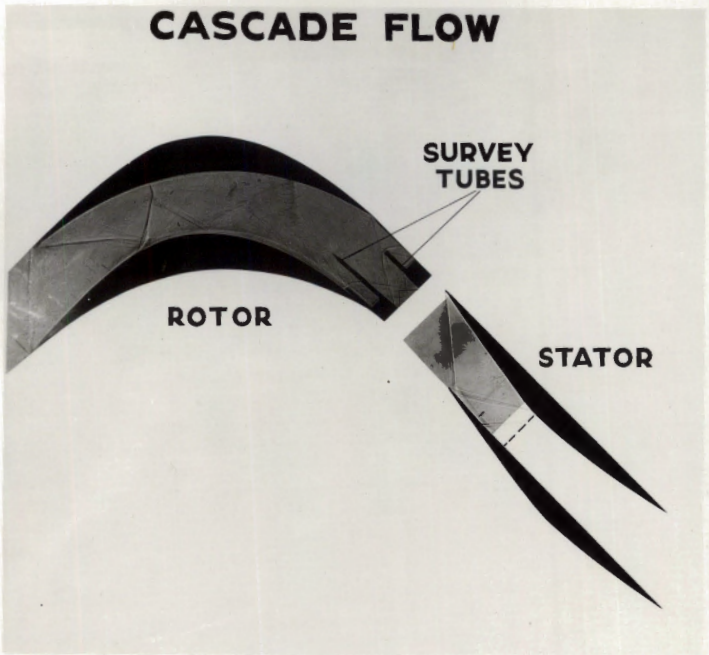

NACA

LAL 61106